Beam optics analysis of large-acceptance superconducting in-flight separator BigRIPS at RIKEN RI Beam Factory (RIBF)

- Magnetic spectrometer used for the production of radioactive isotope (RI) beams based on in-flight scheme
- Objective: study of exotic nuclei far from the stability using a variety of RI beams

Presented by Hiroshi Suzuki

RIKEN Nishina Center

Toshiyuki Kubo, Hiroyuki Takeda,
Kensuke Kusaka, Naohito Inabe,
Naoki Fukuda, & Daisuke Kameda

RIKEN NISHINA CENTER

ICAP2012 @Warnemuende, Germany, Aug. 20, 2012

Outline of My Talk

- Introduction
  - Overview of BigRIPS separator, emphasizing its ion-optics issues
- Optics Calculation
  - Optics Calculation for BigRIPS, which is a large acceptance and large-aperture ion-optical system
    - Field map measurements
    - The procedure to deduce $b_{n,0}(z)$ from magnetic field vector
    - The procedure to fit the Enge function
    - Optics calculation using with COSY INFINITY
- Comparison with Measurement
    - Matrix terms
    - A/Q resolution from New-isotope Search Exp.
- Summary

Introduction

RIBF Layout

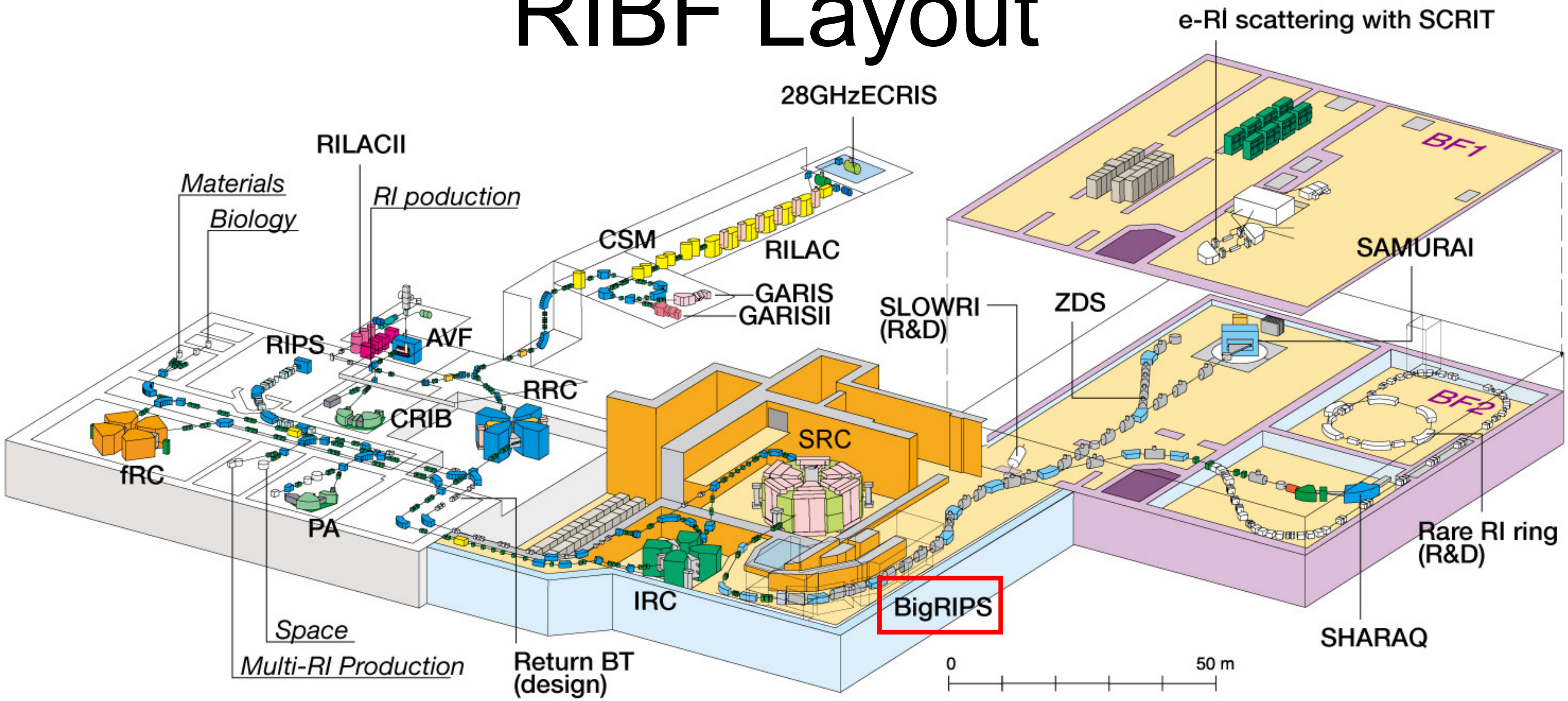

New-generation in-flight RI beam facility, Energy : 345 MeV/u up to ^{238}U ions

Reaction mechanism of RI production

- Projectile fragmentation

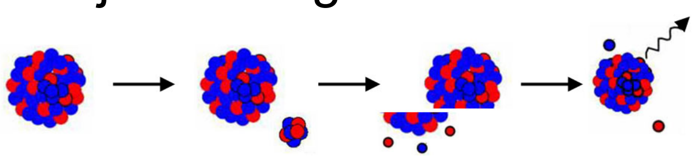

- In-flight fission

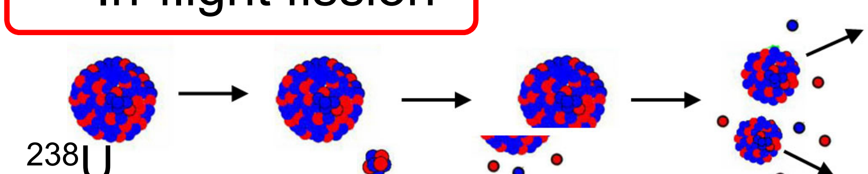

Very powerful for neutron-rich RIs in mid-heavy region

Features of BigRIPS Separator

- 1) Large acceptances
  - Comparable with angular / momentum spreads of in-flight fission at RIBF energy (+/-50 mrad, +/-5%)
- 2) Superconducting quads with a large aperture
  - Pole tip radius: 17 cm
  - Max. pole tip field: 2.4 T
- 3) Two-stage separator scheme
  - 1st stage : 2 bend, p/Δp=1260
  - 2nd stage : 4 bend, mirror sym. @ F5, p/Δp= 3420
  - Better resolution at 2nd stage for particle ID

Parameters:
Δa = +/-40 mrad
Δb = +/-50 mrad
$\Delta p/p$ = +/-3 %
$B\rho$ = 9 Tm
L ~ 77 m

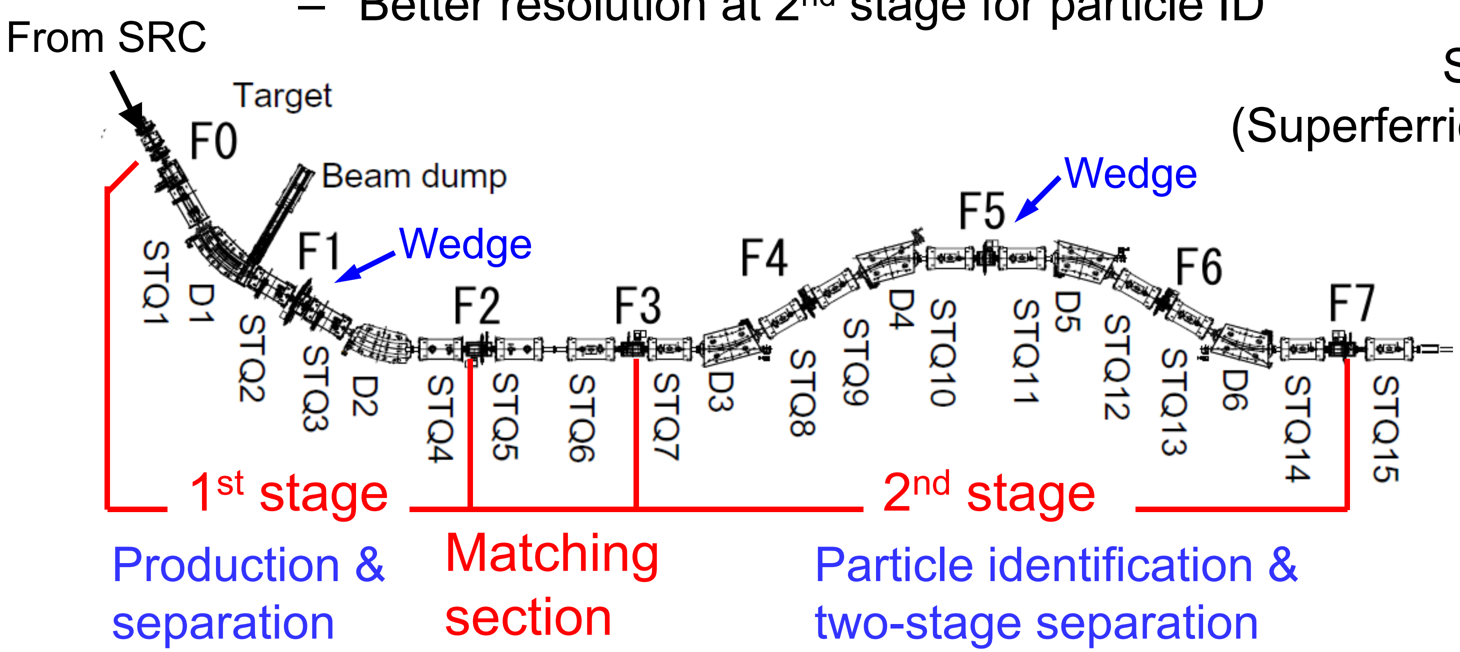

STQ (Superferric Q)

STQ1-14: Superconducting quad. triplets

D1-6: Room temp. dipoles (30 deg)

F1-F7: focuses

Ion Optics of BigRIPS

1st stage   Matching section   2nd stage (Mirror symmetry at F5)

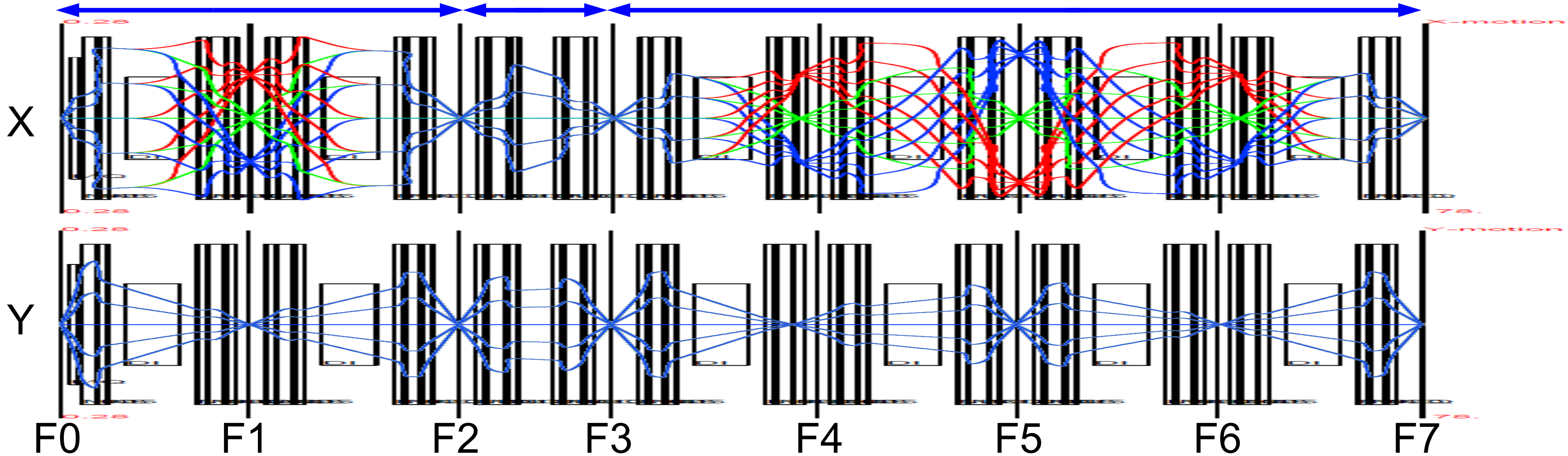

F0F1

(x|x)=-1.7, (x|a)=0,
(y|y)=-5.0, (y|b)=0,
(x|δ)=-21.4 mm/%, (a|δ)=0

F0F2

(x|x)=2.0, (x|a)=0,
(y|y)=1.6, (y|b)=0,
(x|δ)=0 mm/%, (a|δ)=0

F2F3

(x|x)=-1.08, (y|y)=-1.18,
(x|a)=(y|b)=(a|x)=(b|y)=0

F3F4

(x|x)=-1.40, (x|a)=-0.791,
(y|y)=-3.45, (y|b)=-0.272,
(x|δ)=-22.1 mm/%, (a|δ)=0

F3F5

(x|x)=0.92, (x|a)=0,
(y|y)=1.06, (y|b)=0,
(x|δ)=31.7 mm/%, (a|δ)=0

P/ΔP =
1260 (1st stage)
3420 (2nd stage)

Mirror symmetry
of F3-F5

F7F6

F7F5

Large-Aperture, Short-Length Superconducting Quadrupole

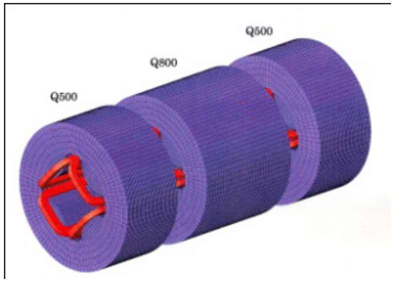

- Superferric (STQ2-26) : iron dominated

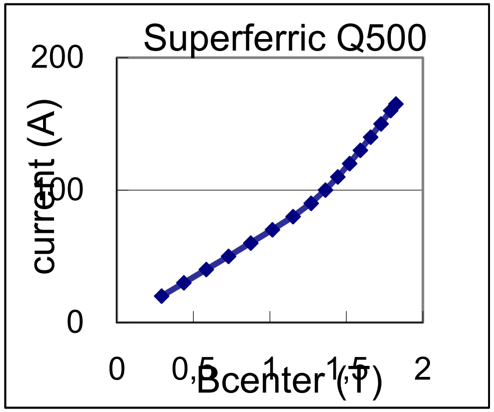

Excitation function

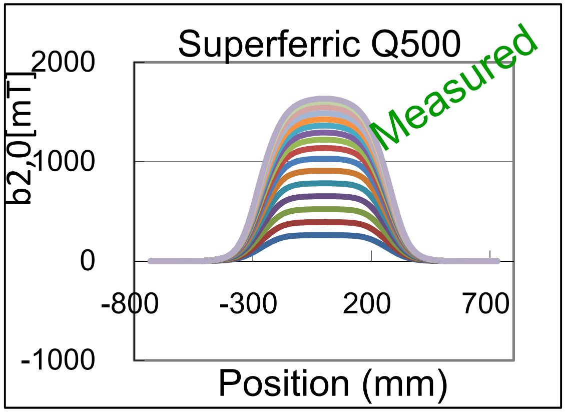

Field distribution

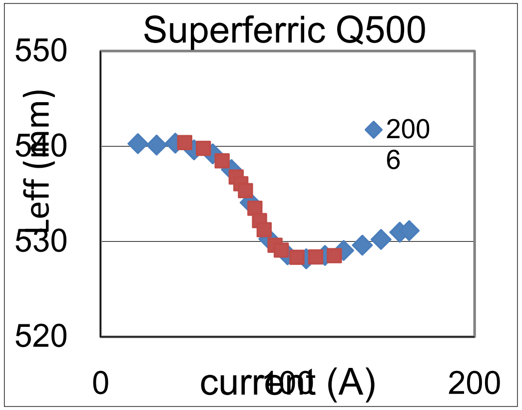

Effective length

Large fringe field regions and saturation effects!

- Air-core (STQ1)

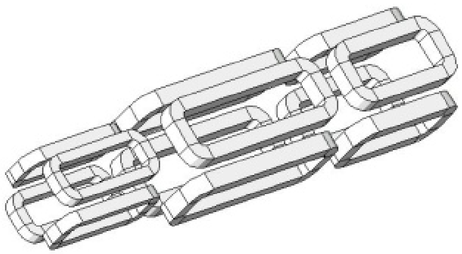

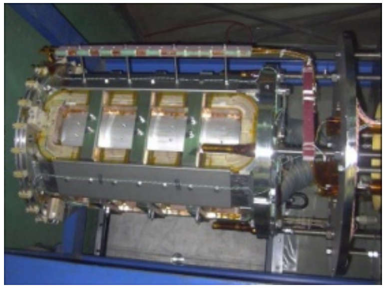

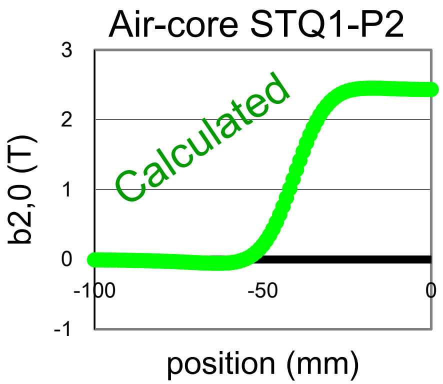

Field distribution

Calculation for Optical Setting

Our goal: precise ion-optical setting, in which tuning is not needed.

Quadurpoles have large fringe field region and strong saturation effects.
The field distribution varies very much with the magnet excitation.

↓

The effect of the varying distribution should be included in the simulation.

Procedure of the field & optics analysis

- Measure detailed field-map as a function of magnet current.
- Deduce $b_{n,0}(z,I)$ from the magnetic field map.
- Fit $b_{n,0}$ distribution by Enge function.
  Its Enge coefficients are the function of magnet current.
- Make detailed ion-optical calculation using the deduced Enge coefficients and COSY INFINITY code.
- Search magnet current setting, which satisfies the ion optical setting.

$$F(z) = \frac{1}{1+\exp\left[a_1 + a_2\left(z/D\right) + \cdots + a_6 (z/D)^5\right]}$$

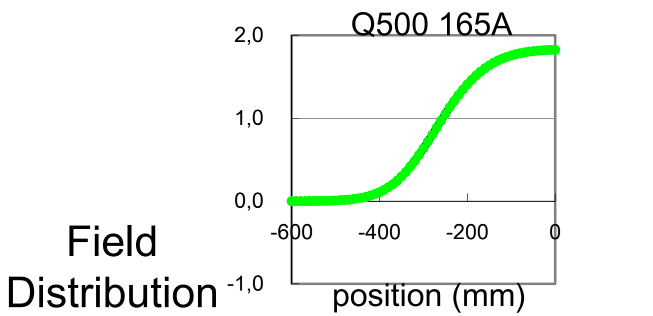

Optics Calculation

Field Map Measurement

- Quadrupole & Sextupole

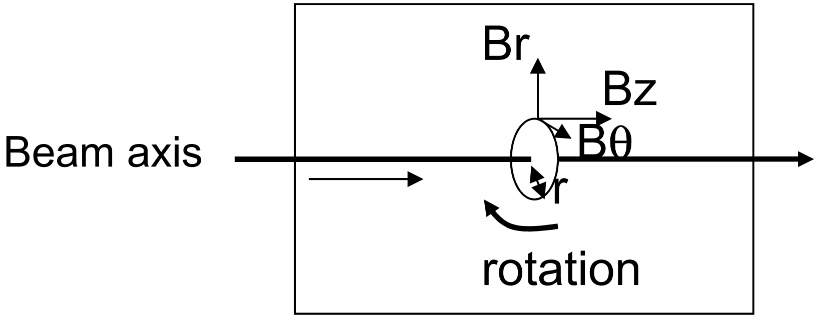

Radius : r = 81,94,107 mm
Step :
Δz = 10 mm
$\Delta\theta$ = 9 degree (for quadrupole)
3 degree (for sextupole)

- Dipole

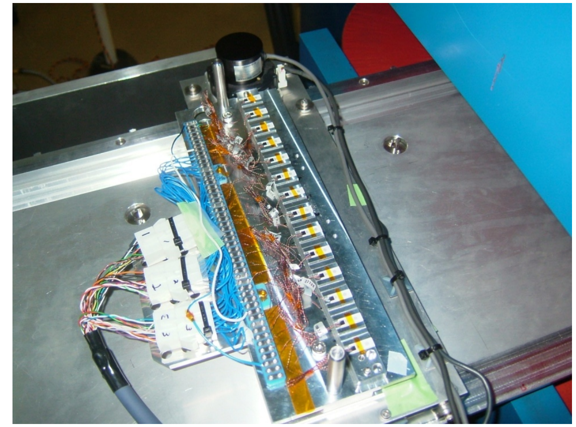

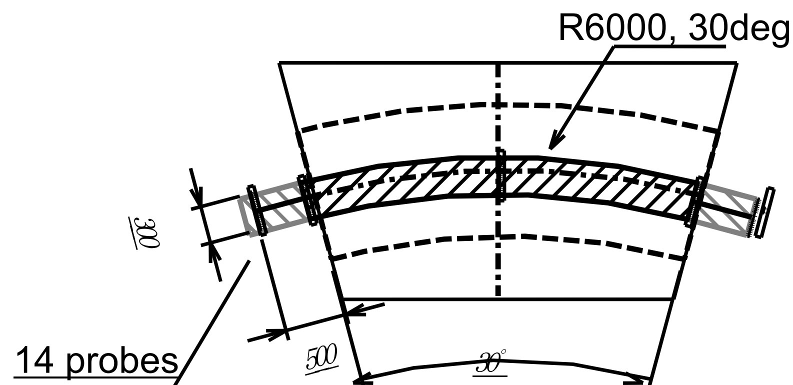

Range : outside +/-500 mm
Step : 20 mm (center : 10 mm)
Plane : mid-plane, +/-10, 20, 30, 40 mm
(Gap : +/-70 mm)

Magnetic Field in θ Direction

Quadrupole

Q500, z=2230mm, I_Q=100A, I_{SX}=0A

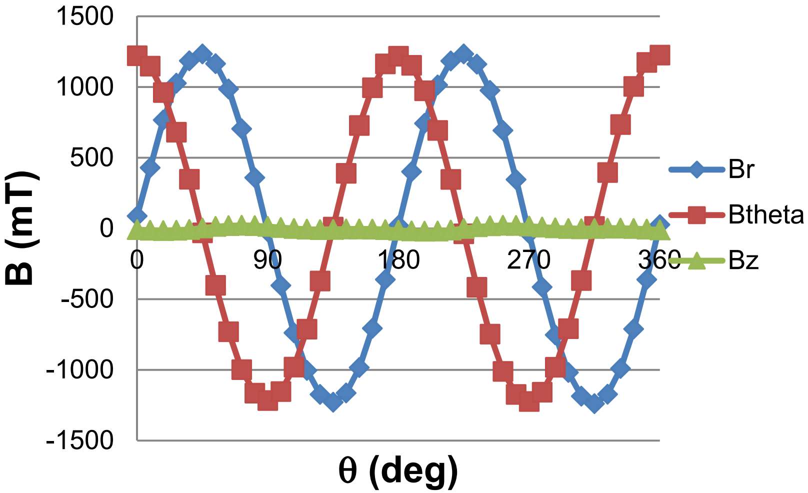

Q500, z=1980mm, I_Q=100A, I_{SX}=0A

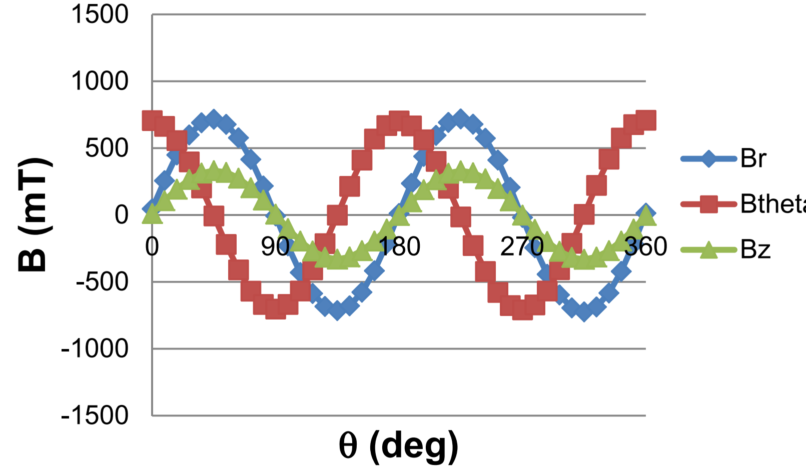

Sextupole

SX, z=2230mm, I_Q=0A, I_{SX}=46A

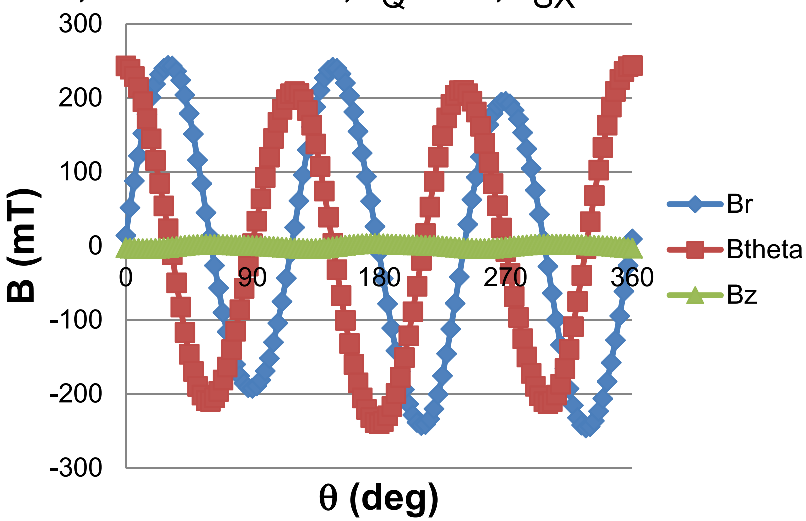

SX, z=1980mm, I_Q=0A, I_{SX}=46A

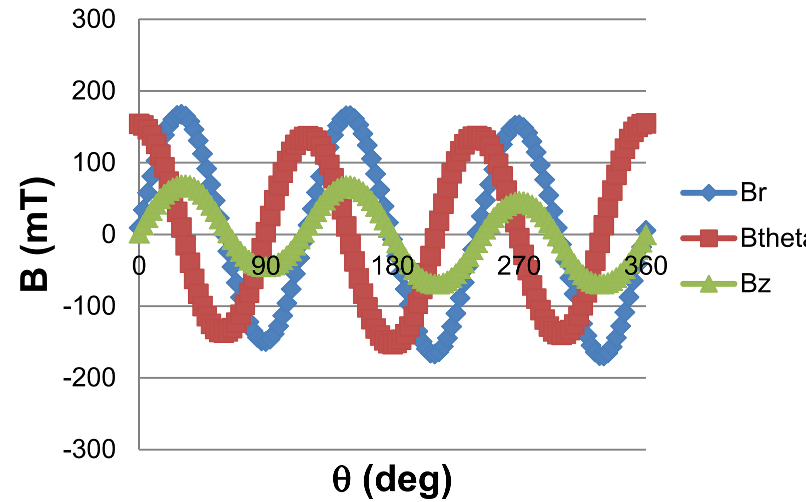

magnet center

field boundary region (edge of mag.)

Multipole Analysis of 3D Mag. Field

Magnetic field vector (B_r, B_θ, $B_z(r,\theta,z)$) is expressed by a scalar $b_{n,0}(z)$.

measurement

1st step (Fourier Analysis)

(w/o skew components)

$$\begin{cases} \boxed{B_r(r,\theta,z)} = \sum_{n=1}^{\infty} \boxed{B_{r,n}(r,z)} \sin n\theta, \\ \boxed{B_\theta(r,\theta,z)} = \sum_{n=1}^{\infty} \boxed{B_{\theta,n}(r,z)} \cos n\theta, \\ \boxed{B_z(r,\theta,z)} = \sum_{n=1}^{\infty} \boxed{B_{z,n}(r,z)} \sin n\theta. \end{cases}$$

n=1: dipole
n=2: quadrupole
n=3: sextupole
…

2nd step (Deducing $b_{n,0}$)

$$\begin{cases} \boxed{B_{r,n}(r,z)} \equiv \left(\frac{r}{r_0}\right)^{n-1} \sum_{m=0}^{\infty} \boxed{b_{n,m}(z)} \left(\frac{r}{r_0}\right)^{2m}, \\ \boxed{B_{\theta,n}(r,z)} \equiv \left(\frac{r}{r_0}\right)^{n-1} \sum_{m=0}^{\infty} \frac{n}{n+2m} \boxed{b_{n,m}(z)} \left(\frac{r}{r_0}\right)^{2m}, \\ \boxed{B_{z,n}(r,z)} \equiv \left(\frac{r}{r_0}\right)^{n} \sum_{m=0}^{\infty} \frac{r_0}{n+2m} \frac{\partial}{\partial z} \boxed{b_{n,m}(z)} \left(\frac{r}{r_0}\right)^{2m}. \end{cases}$$

$$b_{n,m}(z) = -\frac{r_0^2}{4m(n+m)} \frac{n+2m}{n+2(m-1)} \frac{\partial^2}{\partial z^2} b_{n,m-1}(z).$$

Fourier Transform of Differential Eq.

$$b_{n,m}(z) = -\frac{r_0^2}{4m(n+m)} \frac{n+2m}{n+2(m-1)} \frac{\partial^2}{\partial z^2} b_{n,m-1}(z).$$ (m>0)

Fourier transform

$$\boxed{\begin{aligned} &\tilde{b}_{n,m}(k) = \int_{-\infty}^{\infty} b_{n,m}(z) e^{-ikz}\, dz \\ &\frac{\partial}{\partial z} \to -ik \end{aligned}}$$

z derivative can be translated into simple algebraic calculation by FT

$$\begin{aligned}
\tilde{b}_{n,m}(k) &= -\frac{r_0^2}{4m(n+m)} \frac{n+2m}{n+2(m-1)} (-ik)^2\, \tilde{b}_{n,m-1}(k) \\
&= \underbrace{\frac{(r_0 k)^2}{4m(n+m)} \frac{n+2m}{n+2(m-1)}}_{q_m} \tilde{b}_{n,m-1}(k) \\
&= q_m \tilde{b}_{n,m-1}(k) \\
&= q_m q_{m-1} \tilde{b}_{n,m-2}(k) \\
&\vdots \\
&= q_m q_{m-1} \cdots q_1 \tilde{b}_{n,0}(k) \\
&= p_m \tilde{b}_{n,0}(k) \quad \left(p_m \equiv \prod_{i=1}^{m} q_i \right)
\end{aligned}$$

Procedure to Deduce $b_{n,0}$ from $B_{r,n}$

$$B_{r,n}(r,z) = \left(\frac{r}{r_0}\right)^{n-1} \sum_{m=0}^{\infty} b_{n,m}(z) \left(\frac{r}{r_0}\right)^{2m}$$ (diff. eq.)

$$B_{r,n}(r=r_0,z) = \sum_{m=0}^{\infty} b_{n,m}(z)$$ (diff. eq.)

Fourier tr.

$$\tilde{B}_{r,n}(k) = \int_{-\infty}^{\infty} \boxed{B_{r,n}(r=r_0,z)} e^{-ikz}\, dz$$

decomposed from measured data

$$\tilde{B}_{r,n}(k) = \sum_{m=0}^{\infty} \tilde{b}_{n,m}(k) = \sum_{m=0}^{\infty} p_m \tilde{b}_{n,0}(k)$$

$$\tilde{b}_{n,0}(k) = \tilde{B}_{r,n}(k) \Bigg/ \sum_{m=0}^{\infty} p_m$$

$$\tilde{B}_{\theta,n}(k) = \sum_{m=0}^{\infty} \frac{n}{\underline{n+2m}} \tilde{b}_{n,m}(k) = \sum_{m=0}^{\infty} \frac{n}{\underline{n+2m}} p_m \tilde{b}_{n,0}(k)$$

$$\tilde{b}_{n,0}(k) = \tilde{B}_{\theta,n}(k) \Bigg/ \sum_{m=0}^{\infty} \frac{n\, p_m}{\underline{n+2m}}$$

$b_{n,0}$ from $B_{\theta,n}$

Inv. Fourier tr.

$$b_{n,0}(z) = \frac{1}{2\pi} \int_{-\infty}^{\infty} \tilde{b}_{n,0}(k) e^{+ikz}\, dk$$

Using the procedure of Fourier tr. and inverted Fourier tr., $b_{n,0}(z)$ is obtained from $B_{r,n}(r,z)$, without solving the high differential equation.

$b_{2,0}(z)$ Distribution along the Axis

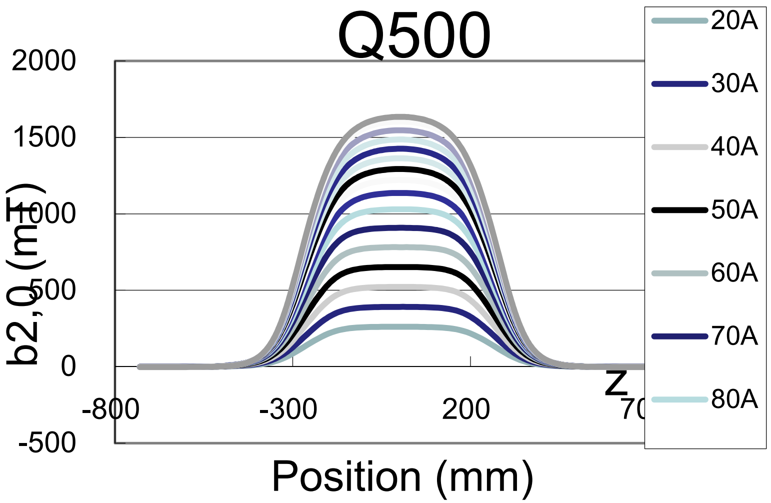

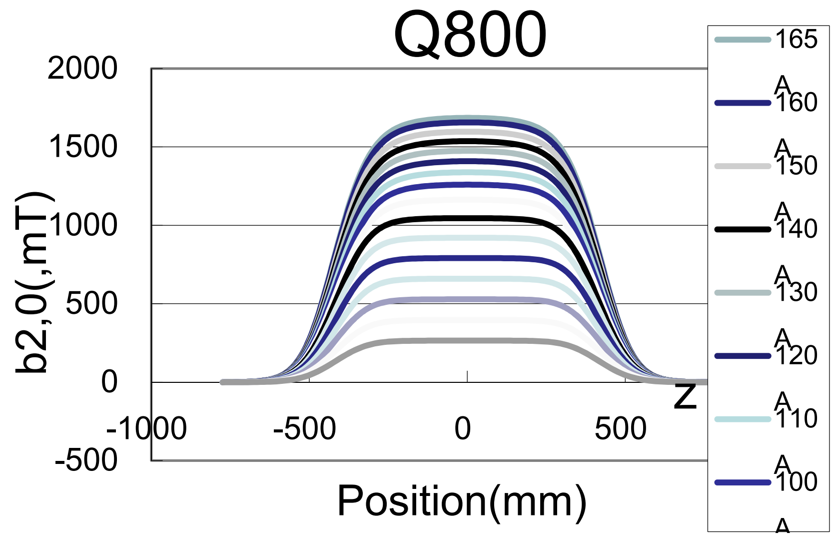

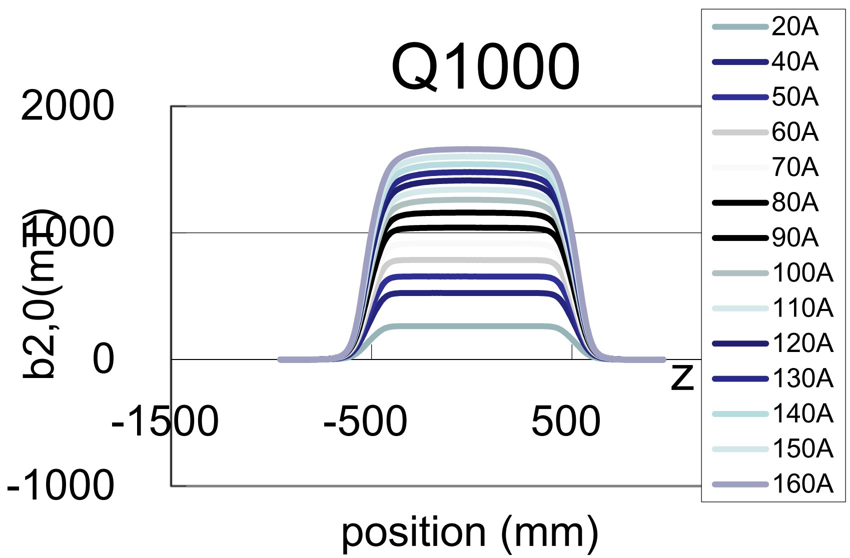

Deduced from B_r (r=107 mm)

- The fringe region is very large.
- The shape of the distribution varies much with the excitation.

Enge Function for Fringe of $b_{n,0}$

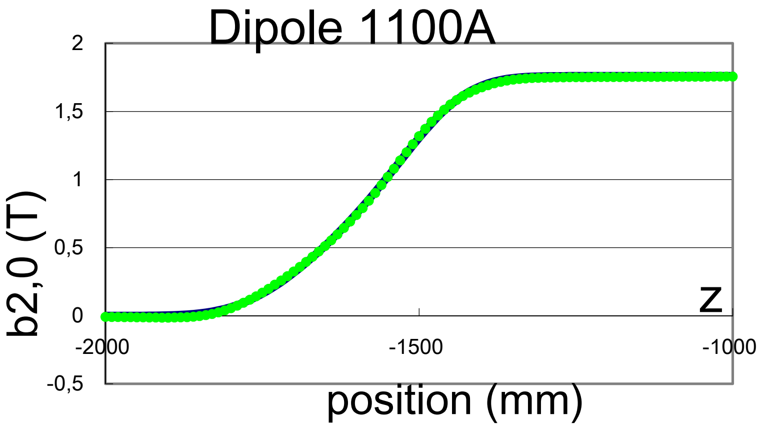

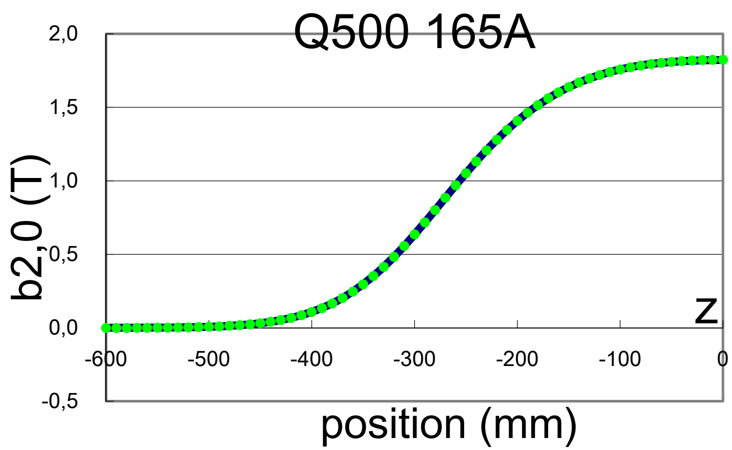

$$F(z) = \frac{1}{1 + \exp\left(a_1 + a_2(z/D) + \cdots + a_6(z/D)^5\right)}$$

D : Pole tip diameter

a_1-a_6 : parameter

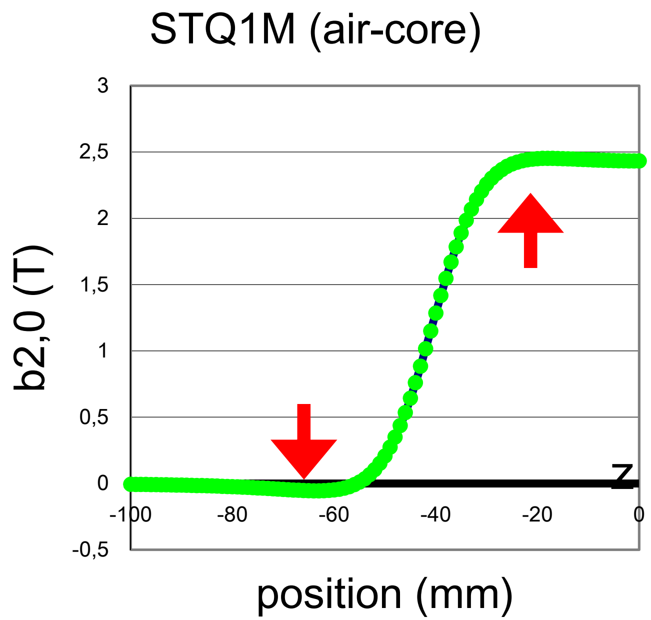

Overshooting & undershooting part

→Second term is introduced (a_7-a_{11})

$$F(z) = \frac{1}{1 + \exp\left(a_1 + a_2(z/D) + \cdots + a_6(z/D)^5\right)} + a_7 \times \tanh\left(a_8 + a_9(z/D)\right) \times \exp\left(-\frac{\left((z/D) + a_{10}\right)^2}{a_{11}^2}\right)$$

Enge Coefficients

As a function of magnet current (Q500, inner side)

$a_1(I)$

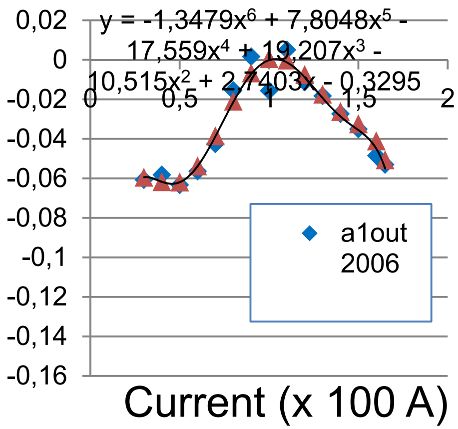

$a_2(I)$

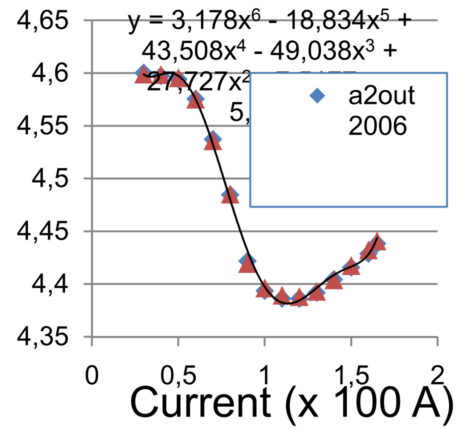

$a_3(I)$

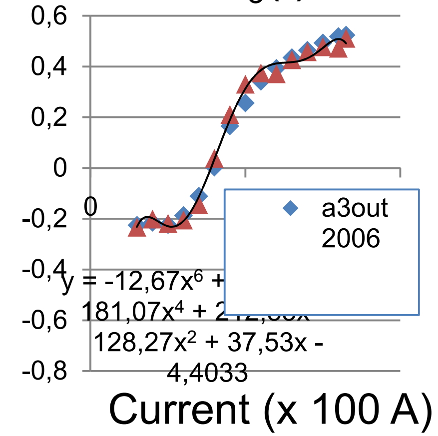

$a_4(I)$

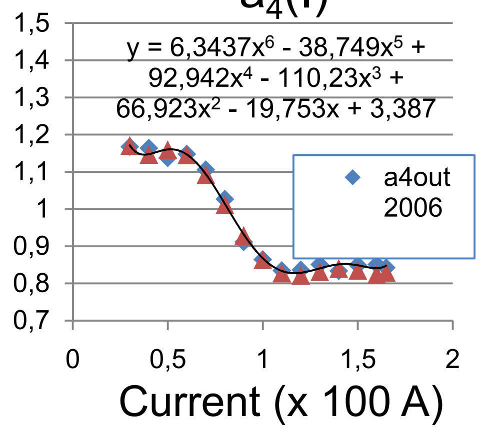

$a_5(I)$

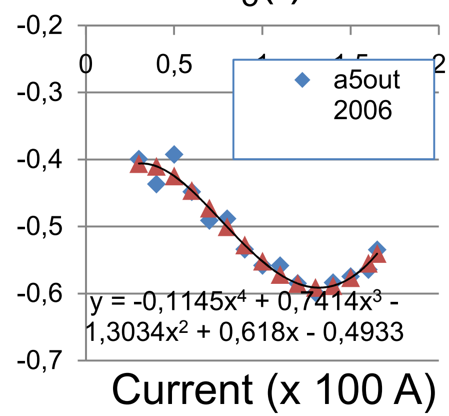

$a_6(I)$

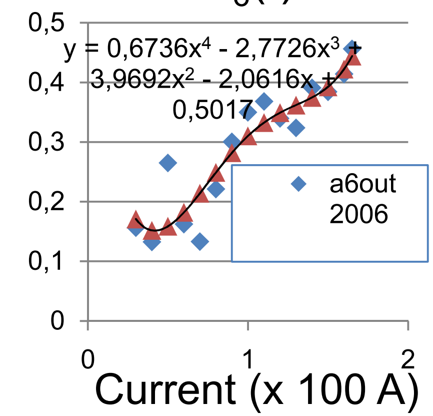

Enge coefficients are fitted with polynominal function.
→ Fitted Enge coefficients are used in our optics calculation.

Optics Search using COSY INFINITY

- Optics search using symplectic transfer maps that allow symplectic scaling is made.
- Symplectic transfer maps are calculated beforehand using the fitted Enge coefficients for discrete values of magnet current (see the lower plot).
- During the search, symplectic transfer maps whose magnet current is closest are chosen and used for optics calculation applying the symplectic scaling.
- This scheme allows fast search, saving computational time.

e.g. a_2 for Q500 outer side

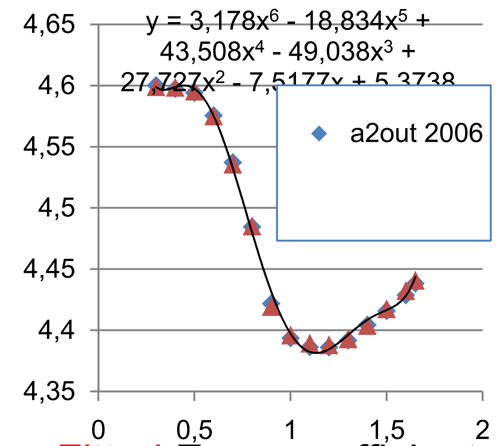

Fitted Enge coefficients

Symplectic transfer maps are calculated for the points below.

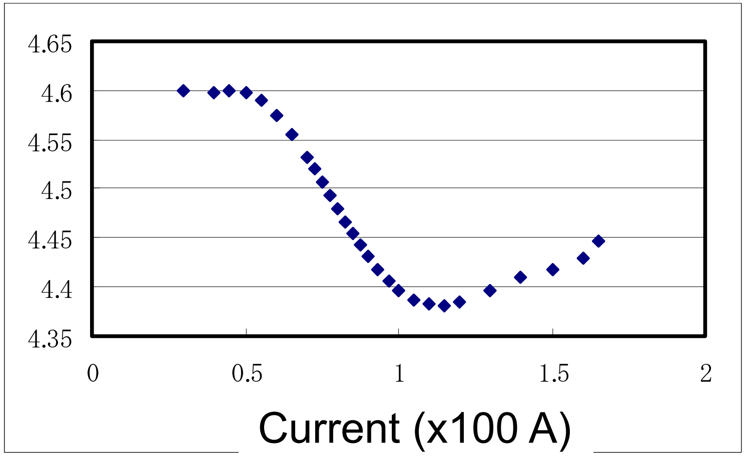

Comparison with measurements

Determination of matrix terms from 2ndary beam

1st order matrix elements from F3 to F5

(x|x)

F5x vs F3x correlation

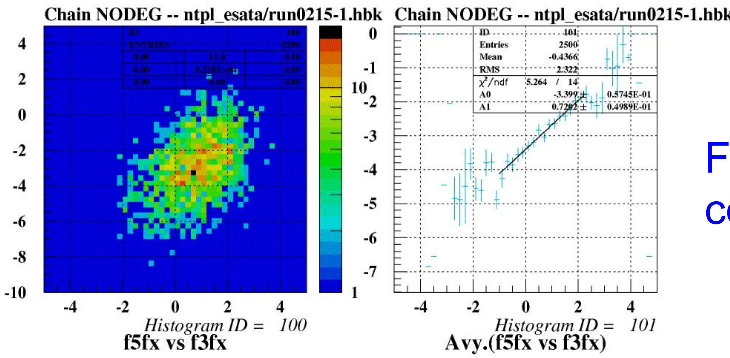

(a|x)

F5a vs F3x correlation

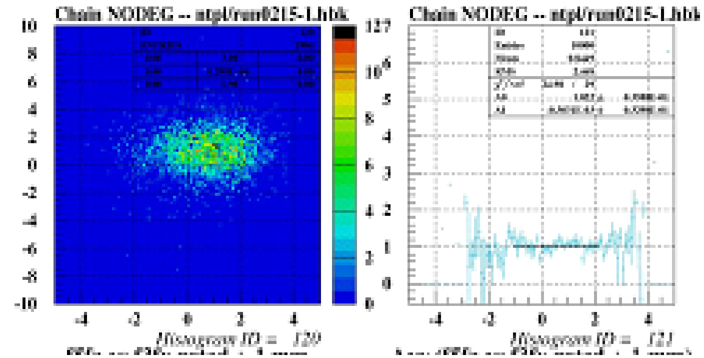

(x|a)

F5x vs F3a correlation

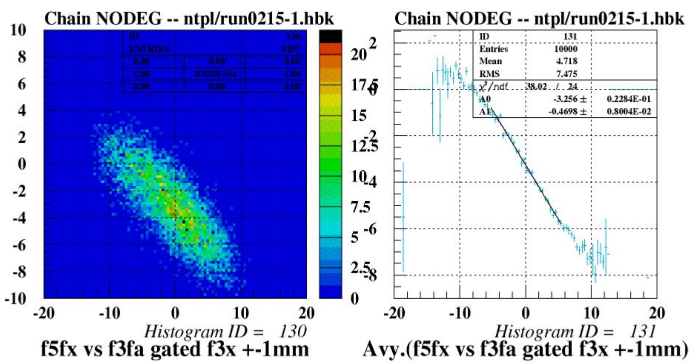

(a|a)

F5a vs F3a correlation

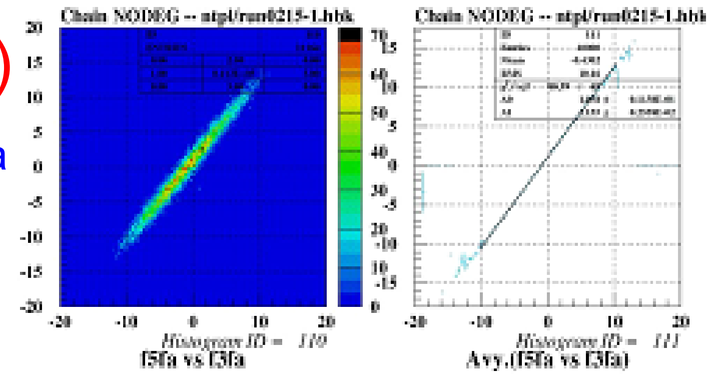

(x|δ)

F5x vs TOF correlation

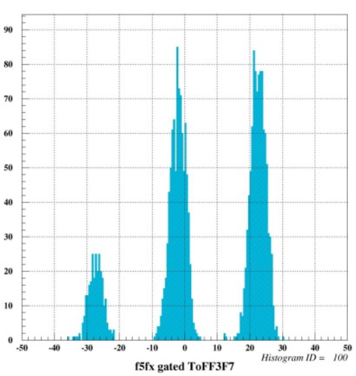

90Br is selected (produced by in-fight fission).

(a|δ)

F5a vs TOF correlation

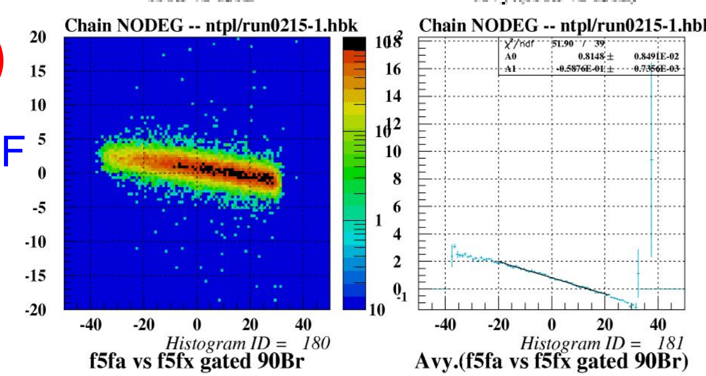

F3x: ±1mm, F3a: ±1mrad gates are applied. δ is gated with TOF37: ±1ns.

Comparison for the matrix terms

(x|x)

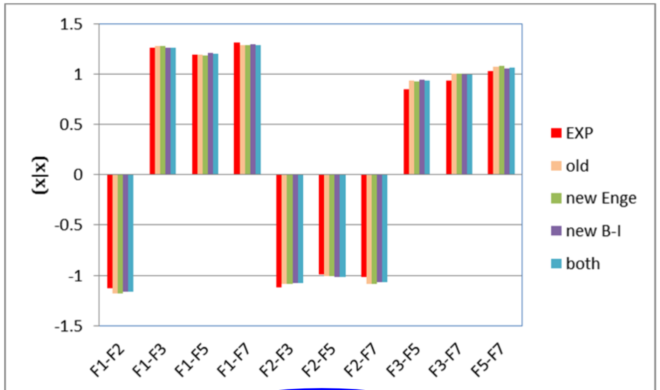

(a|x)

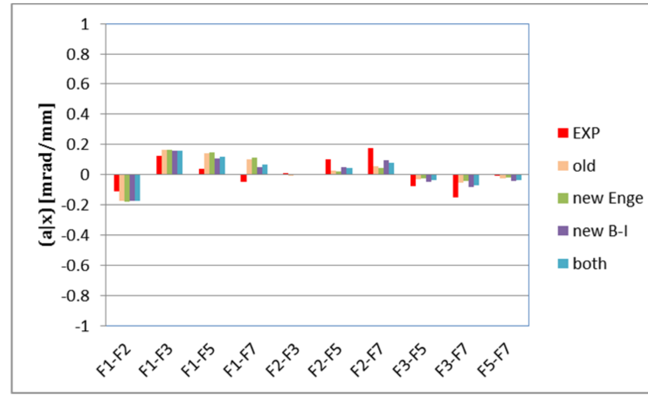

measured

(x|a)

Focusing term

Not sufficient…

(a|a)

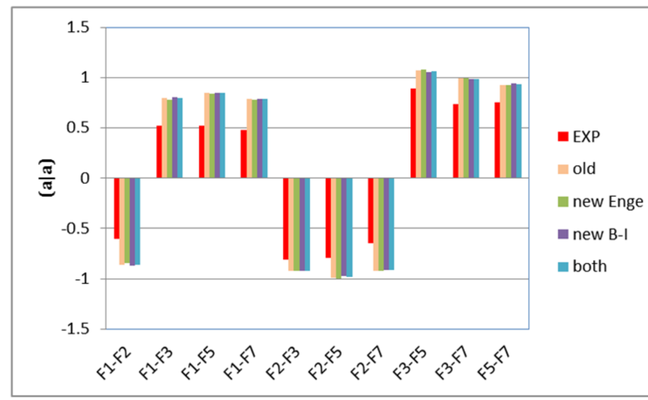

(x|δ)

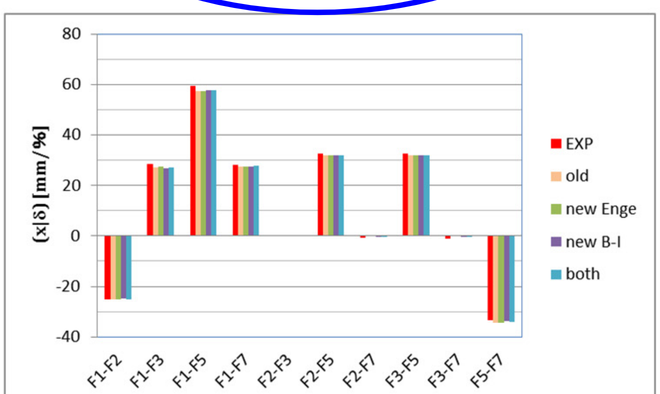

(a|δ)

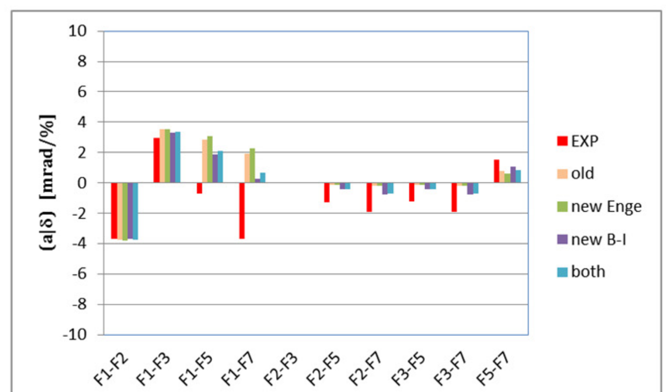

Particle Identification in 2nd Stage

TOF-Bρ-ΔE method with track reconstruction

→ Improve the Bρ and TOF resolution

Measure β, Bρ, ΔE @ 2nd stage

+ isomeric γ-rays

Z, A/Q

$$Z \leftarrow -dE/dx = f(Z,\beta)$$

$$A/Q = \frac{B\rho}{c\beta\gamma}$$

- Bρ ← by track reconstruction.
  - x_3, a_3, x_5, a_5 → $B\rho_{35}$
  - x_7, a_7, x_5, a_5 → $B\rho_{57}$ (ion optics)
- β ← by the couple equations.
  - $TOF_{37} = L_{35}/\beta_{35}c + L_{57}/\beta_{57}c$
  - $A/Q = B\rho_{35} / c\beta_{35}\gamma_{35}$
  - $A/Q = B\rho_{57} / c\beta_{57}\gamma_{57}$

a: θ(angle in horizontal)

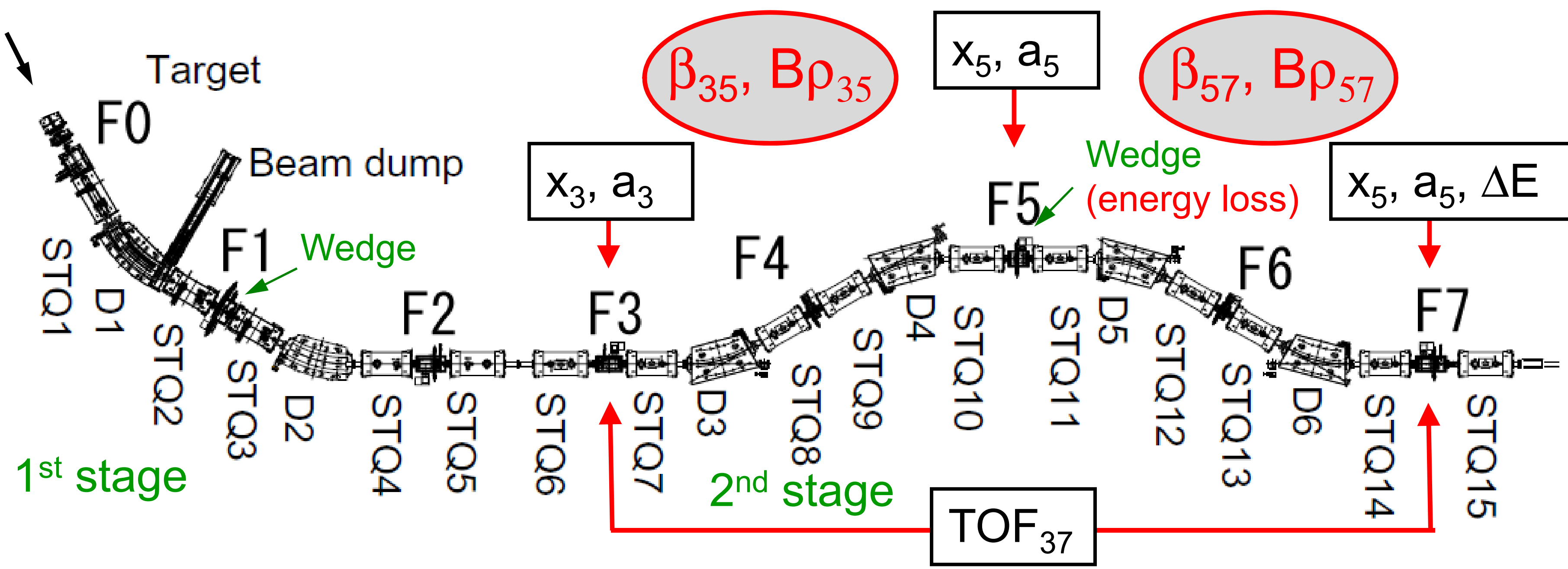

PID Power for Fission Fragments

High enough to well identify charge states.
thanks to the track reconstruction!

Z vs. A/Q plot

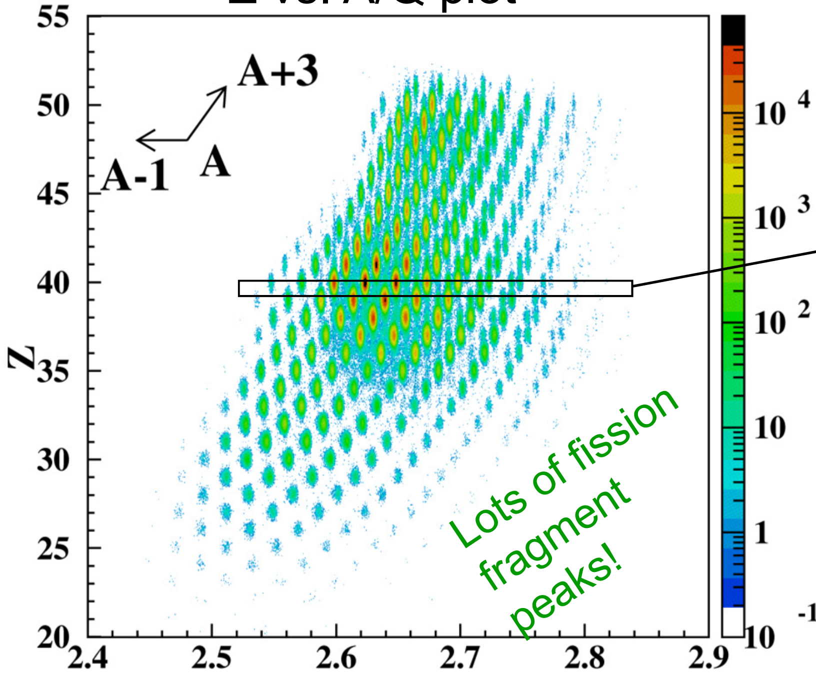

ΔP/P =+- 3%

A/Q spectrum for Zr isotopes (Z=40)

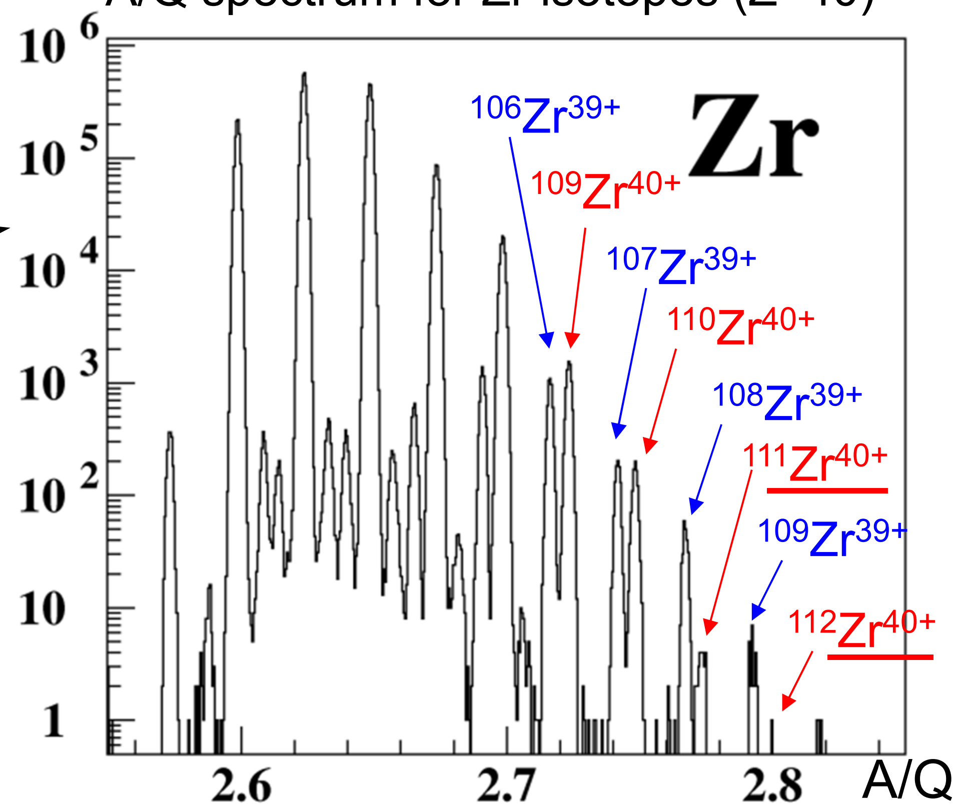

U-beam+2.9-mm Be, Bρ01 = 7.990 Tm
F1 deg: 2.18-mm Al, Δp/p: +/-3%, G3 setting (Z~40)
J. Phys. Soc. Jpn. 79 (2010) 073201.

r.m.s. A/Q resolution: 0.035 %

Improvement of PID Power

Sn isotopes produced by in-flight fission of ^{238}U

Up to 1st order (calc.)

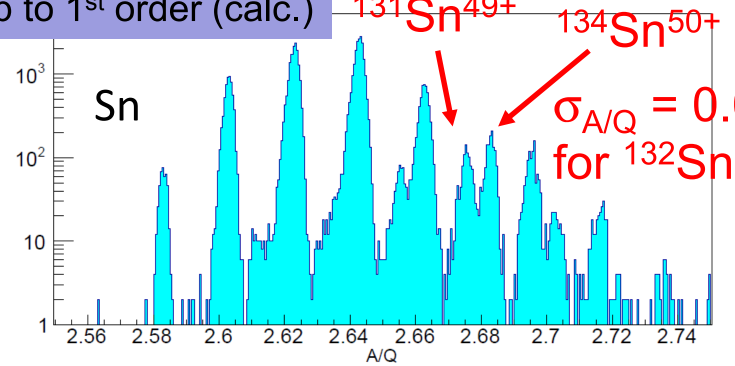

$\sigma_{A/Q}$ = 0.058% for $^{132}Sn^{50+}$

Up to 3rd order (calc.)

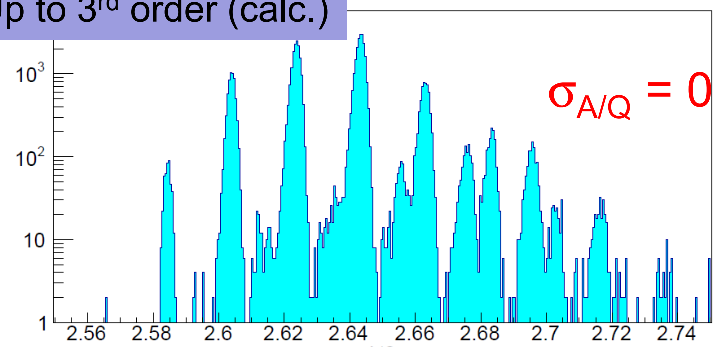

$\sigma_{A/Q}$ = 0.050%

Up to 3rd order (deduced from exp.)

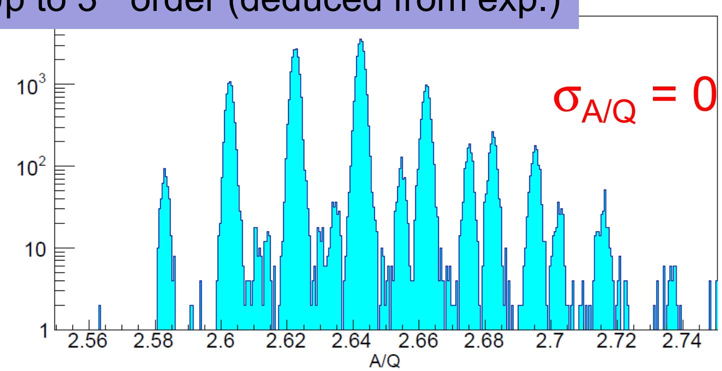

$\sigma_{A/Q}$ = 0.041%

A/Q

Reconstructed δ and F3a vs A/Q

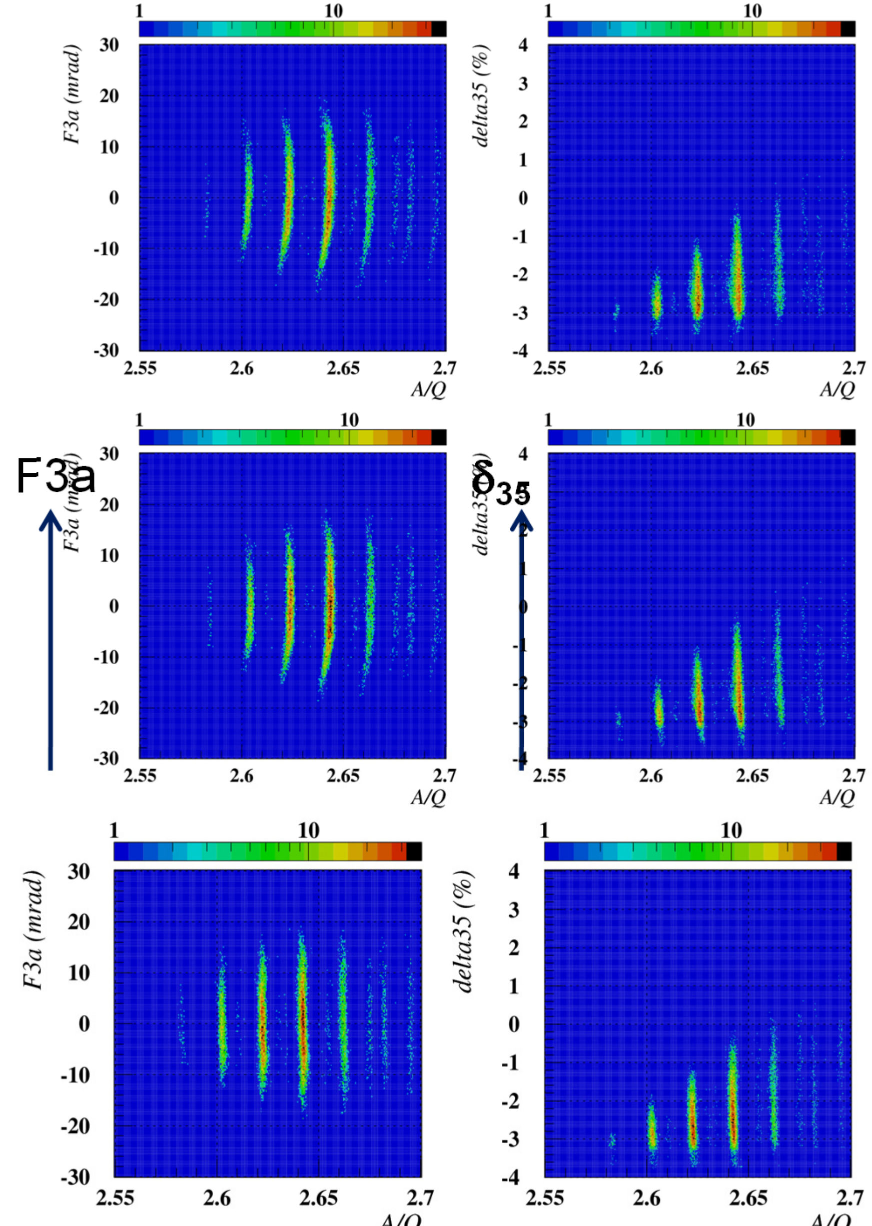

Issues

- COSY predictability improvement
  - Improvement of magnetic field measurement
    - Magnetic field distribution
    - Cross talk between Q and SX (not only Q→SX but also SX→Q)
  - Better analysis of measured magnetic field-maps
    - B-I curve quality
    - Fitting $b_{n,0}$ distribution with Enge function (the function of z)
    - Fitting Enge coefficient (the function of I)

→ allowing us to achieve our goal: precise optics setting, in which any tuning is not needed.

→ allowing us to achieve excellent track reconstruction without using experimentally-determined transfer maps.

Summary

- Introduction
  - BigRIPS has large acceptance and large aperture for the fission fragments of ^{238}U beam.
  - For this feature, Superconducting quadrupoles are used.
  - The field distribution of STQ varies very much with the magnet excitation.
- Optics Calculation
  - Goal: precise ion-optical setting is calculated, in which tuning is not needed.
  - To achieve this goal, the varying field distribution should be included in the optics calculation.
  - The procedure of the magnetic field analysis is shown.
  - For deducing $b_{n,0}$, a new approach using Fourier Transform is shown.
- Comparison with measurement
  - Matrix term: the agreement of $(x|a)$ term is not sufficient.
  - A/Q resolution: there is room for improvement.

Thank you for your attention!